ISSN 1027-5495. Functional Materials, 33, No.1 (2026), p. 24-32
doi:http://dx.doi.org/10.15407/fm33.01.24 © 2026 — STC "Institute for Single Crystals"
This is an open access article under the CC BY-NC-ND license (http://creativecommons.org/licenses/by-nc-nd/4.0/).

Prediction of spin-polarization characteristics of Al@Si -doped single-walled (6,0) SiC nanotubes

Vusala Nabi Jafarova[1], A.A. Hadiyeva[1,2*], V.K. Sarijanova[1], Sh.R.Mammadova[1], A.K. Sijo[3], Merin Sabi[4]

[1] Azerbaijan State Oil and Industry University, 20 Azalig Ave., AZ-1010, Baku, Azerbaijan
[2] Khazar University, 41 Mehseti Str, AZ1096 Baku, Azerbaijan
[3] Department of Physics, Mary Matha Arts and Science College, Mananthavady, Kannur University, Kerala, India-670645
[4] Department of Chemistry, Nirmalagiri College, Kannur Kerala, India, 670701
*e-mail: aynura.hadiyeva@asoiu.edu.az

Received September 5, 2025, approved February 7, 2026

In this study, we examine the impact of aluminum substitution on the structural, electronic, and magnetic properties of single-walled (6,0) silicon carbide nanotubes using spin-polarized density functional theory calculations. The introduction of Al into the nanotube lattice significantly alters its electronic structure, leading to a transition toward half-metallic behavior. Specifically, the spin-up channel retains a semiconducting nature, while the spin-down channel becomes metallic, indicating a clear spin-dependent conductivity. The partial density of states analysis reveals that the electronic states near the Fermi level are dominated by carbon p-orbitals, with additional contributions from the d-orbitals of the aluminum dopant. Spin-resolved charge density distributions further show the emergence of a net magnetic moment of approximately 1.0 μ_B, which is mainly localized on the carbon atoms adjacent to the Al impurity. A comparison of total energies for ferromagnetic and antiferromagnetic configurations indicates that the antiferromagnetic state is energetically more stable and therefore represents the ground state of the system. Taken together, these findings suggest that Al@Si-doped (6,0) SiC nanotubes possess a combination of half-metallic characteristics and stable magnetic ordering, making them promising materials for spintronic applications such as spin filters and antiferromagnetic memory devices.

Keywords: Al-doped SiC, nanotube, ferromagnetic, half-metallic

Прогнозування характеристик спін-поляризації одностінних (6.0) SiC нанотрубок, легованих Al@Si. *V.N. Jafarova. A.A. Hadiyeva, V.K. Sarijanova, Sh.R.Mammadova*

У цьому дослідженні ми розглядаємо вплив заміщення алюмінію на структурні, електронні та магнітні властивості одностінних (6,0) карбід-кремнієвих нанотрубок за допомогою розрахунків теорії спін-поляризованого функціоналу густини. Введення Al у решітку нанотрубки суттєво змінює її електронну структуру, що призводить до переходу до напівметалевої поведінки. Зокрема, канал зі спіном угору зберігає напівпровідниковий характер, тоді як канал зі спіном униз стає металевим, що вказує на чітку спін-залежну провідність. Аналіз часткової густини станів показує, що електронні стани поблизу рівня Фермі переважають вуглецеві p-орбіталі, з додатковим внеском від d-орбіталей легуючої

домішки алюмінію. Розподіл густини заряду з роздільною здатністю за спіном також показує появу чистого магнітного моменту приблизно 1,0 μB, який переважно локалізований на атомах вуглецю, що прилягають до домішки Al. Порівняння повних енергій для феромагнітної та антиферомагнітної конфігурацій вказує на те, що антиферомагнітний стан є енергетично стабільнішим і тому представляє основний стан системи. У сукупності ці результати свідчать про те, що леговані Al@Si (6,0) нанотрубки SiC мають поєднання напівметалевих характеристик та стабільного магнітного впорядкування, що робить їх перспективними матеріалами для спінтроніки, таких як спінові фільтри та антиферомагнітні пристрої пам'яті.

1. Introduction

Over the past decade, graphene-inspired two-dimensional semiconductor materials have attracted considerable attention due to their unique structural, chemical, and electronic properties. These characteristics make them highly promising for next-generation spintronic and optoelectronic applications [1,2]. Among such materials, silicon carbide (SiC) has emerged as an important third-generation wide-bandgap semiconductor. It combines a large band gap with excellent thermal conductivity, chemical resistance, and mechanical robustness. Owing to these advantages, SiC has been widely utilized in high-temperature, high-frequency, and high-power electronic devices operating under extreme conditions [2–4]. In addition to electronic applications, SiC nanostructures have also demonstrated potential in biomedical sensing, biocompatible systems, and energy-harvesting technologies [5].

Both theoretical predictions and experimental observations indicate that silicon carbide nanotubes (SiCNTs) exhibit enhanced stability in their electronic and magnetic behavior compared to conventional carbon nanotubes (CNTs) [6–10]. To further expand the functional versatility of Si-based nanostructures in one-, two-, and three-dimensional forms, impurity doping has been extensively explored as an effective approach to tailor their electronic structure and magnetic response. In particular, single-walled SiCNTs doped with metallic or transition-metal elements have been proposed as promising materials for chemical sensing, hydrogen storage, and nanoscale spintronic devices. Such dopants typically induce charge redistribution within the lattice, and the interaction between impurity orbitals and host electronic states can promote magnetic ordering in semiconductor nanostructures [11,12]. For instance, rare-earth doping in chalcogenide systems such as Nd-doped $ZnGa_2Se_4$ has been shown to significantly modify both magnetic response and optical properties due to impurity-induced electronic interactions [12]. For example, previous studies have shown that cobalt incorporation can transform cubic SiC into a metallic phase, while Mn- and Fe-doped (8,0) SiCNTs exhibit half-metallic behavior, which is attractive for spintronic device design [13,14]. Additional density functional theory (DFT) investigations have confirmed that various SiCNT chiralities maintain semiconducting band gaps, highlighting their adaptability for controlled functional modification [15].

Given the similar valence electron configurations of silicon and carbon, the formation of fullerene-like and tubular SiC structures, including the chiral (6,0) nanotube, has long been theoretically anticipated. More recently, first-principles calculations—some combined with machine learning techniques—have demonstrated that noble-metal doping (such as Ag and Au) can effectively tune the magnetic properties of SiCNTs, further supporting their potential in spintronic device engineering [16–19].

In this context, the present study concentrates on aluminum as a group-III dopant. Substituting Al into the SiC nanotube lattice is particularly intriguing because it can modify the electronic and magnetic characteristics in a manner distinct from transition-metal doping. A deeper understanding of these effects may contribute to the rational design of nanoscale devices with enhanced spin-dependent performance and structural stability. Considering that relatively few studies have addressed Al-doped SiCNT systems at Si site, this work aims to clarify the role of aluminum substitution and to broaden the current understanding of doping-induced modifications in SiC-based nanomaterials [20].

2. Computational Methodology

In this work, spin-polarized first-principles calculations were performed within the framework of Density Functional Theory (DFT) to investigate the electronic and magnetic properties of aluminum-silicon substituted single-walled silicon carbide nanotubes (SWSiCNTs) with a (6,0) zigzag configuration. The calculated nanotube diameter was 4.70 Å, consistent with previously reported theoretical values.

The (6,0) SWSiCNT was constructed by rolling a two-dimensional hexagonal SiC monolayer along the chiral vector $C_? = 6a_1 + 0a_2$, corresponding to a zigzag configuration. This rolling procedure transforms the planar SiC sheet into a quasi-one-dimensional tubular structure with well-defined curvature effects. Periodic boundary conditions were applied strictly along the nanotube axis (z-direction) to model an infinitely long nanotube. In contrast, non-periodic boundary conditions were applied in the radial (x and y) directions. To eliminate artificial interactions between neighboring periodic images, a vacuum spacing of at least 15 Å was introduced in both transverse directions. This vacuum thickness was carefully tested to ensure convergence of total energy and electronic properties. The curvature-induced strain and bond rehybridization effects were fully taken into account through complete structural relaxation. During geometry optimization, both atomic positions and lattice parameters along the tube axis were allowed to relax. The optimized diameter and bond lengths were extracted after convergence and remained consistent with theoretical literature values for narrow (6,0) SiCNTs.

All simulations were carried out using the Quantum Atomistix ToolKit (ATK) package, which employs localized numerical atomic orbitals combined with norm-conserving Fritz Haber Institute (FHI) pseudopotentials to describe electron–ion interactions. Exchange–correlation effects were treated within the Local Spin Density Approximation (LSDA). Since LSDA is known to underestimate band gaps in semiconductors, a Hubbard on-site Coulomb correction (LSDA+U) [19, 20] was introduced to better describe localized electronic states and improve the accuracy of magnetic predictions. The effective Hubbard parameters were set to: U_{Si} = 5.0 eV for Si 3d states and U_C = 4.8 eV for C 2p states. These values were selected to reproduce experimentally consistent band gap characteristics of bulk SiC and ensure reliable spin polarization results. The simulation supercell consisted of 24 atoms per primitive unit cell of the (6,0) SiCNT. Aluminum doping was introduced substitutionally by replacing one silicon atom with an Al atom, corresponding to a doping concentration of approximately 8.3 % and 16.6 %.

In this study, geometry optimization was performed until the residual atomic forces were reduced below 0.001 eV/Å and the stress tensor components were minimized to values lower than 0.001 eV/Å^3. The valence electron configurations explicitly considered in the calculations were [Ne] $3s^23p^2$ for silicon (4 valence electrons), [He] $2s^2p^2$ for carbon (4 valence electrons), and [Ne] $3s^23p^1$ for aluminum (3 valence electrons). The Brillouin zone was sampled using a 1×1×5 Monkhorst–Pack k-point grid along the nanotube axis, ensuring convergence of total energy and electronic structure. Spin-resolved band structures and density of states (DOS) were calculated to evaluate spin polarization near the Fermi level. Mulliken population analysis was used to determine atomic magnetic moments and orbital contributions. Furthermore, spin-polarized charge density distributions were visualized to analyze the spatial localization of magnetic states induced by Al substitution and to understand the microscopic origin of spin polarization.

To accurately determine the magnetic ground state, multiple spin configurations were considered, including ferromagnetic (FM) and antiferromagnetic (AFM) alignments. For the FM configuration, the dopants were aligned with parallel spins $Al^{\uparrow}_{x/2}$; $Al^{\uparrow}_{x/2}$, while for the AFM configuration, the dopants had antiparallel spins $Al^{\uparrow}_{x/2}$; $Al^{\downarrow}_{x/2}$. Total energy comparisons were performed to identify the most stable magnetic ordering.

Figure 1 shows the complete computational strategy employed to investigate the structural, electronic, and magnetic properties of Al-doped (6,0) SWSiCNTs. The workflow begins with nanotube construction and structural optimization, followed by doping implementation and magnetic configuration comparison. Subsequent spin-polarized band structure and density of states analyses are performed to evaluate spin polarization, while Mulliken population and spin density mapping provide insight into magnetic behavior. Finally, formation energy calculations are conducted to assess thermodynamic stability and potential applicability in spintronic devices.

3. Results and Discussion

3.1. Electronic characteristics of *SW*SiC:Al nanotubes

This section examines how substitutional aluminum affects the electronic properties of the (6,0) single-walled SiC nanotube. After structural relaxation, the pristine nanotube exhibits a Si–C bond length of approximately 1.88 Å and an average radius of about 3.11 Å, con-

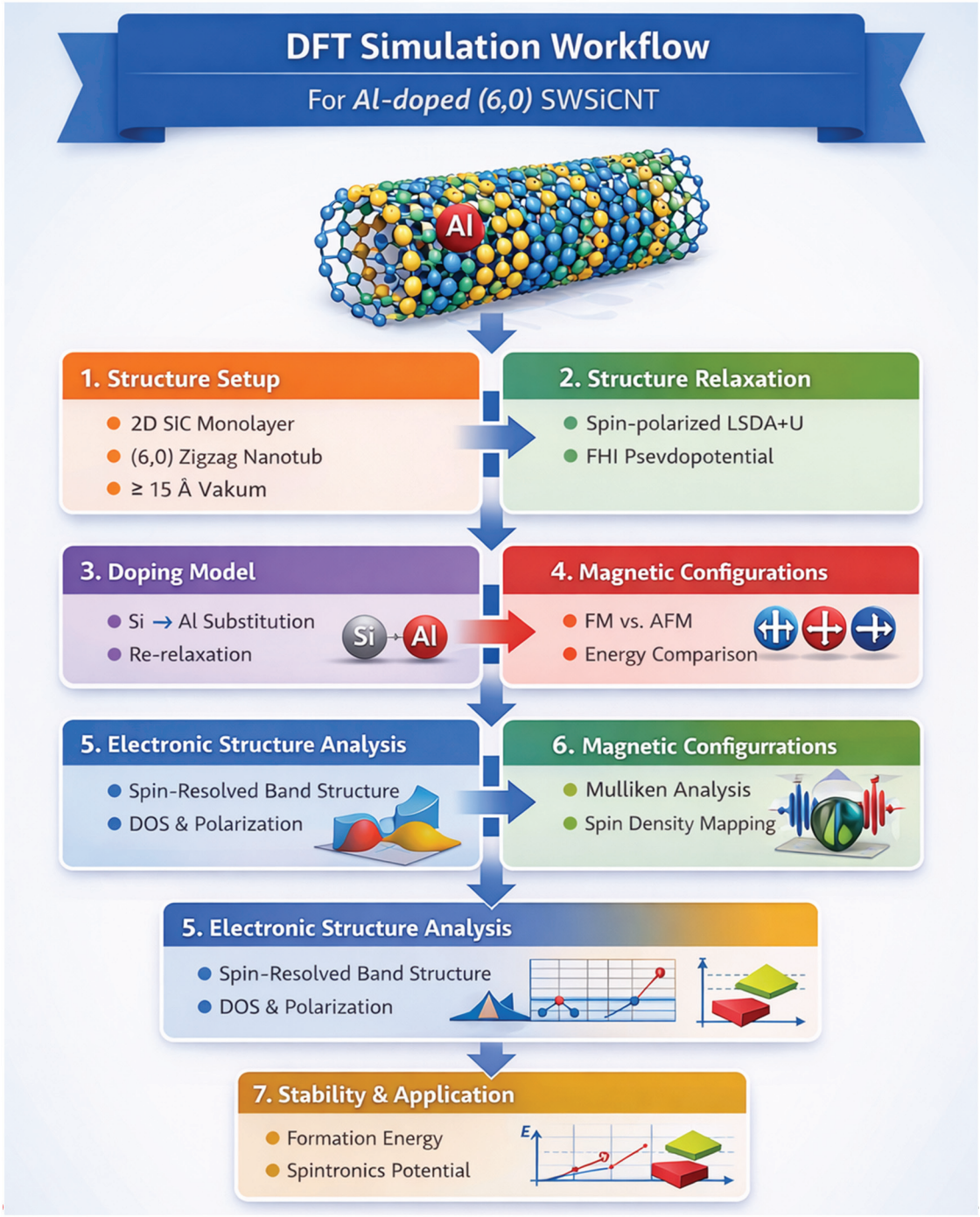

Fig. 1. DFT simulation workflow for Al-doped (6,0) single-walled silicon carbide nanotubes (SWSiCNTs).

firming that the optimized geometry remains structurally stable and symmetric.

When one Si atom is replaced by Al, the electronic structure changes markedly, especially in the spin-resolved states. Spin-polarized band structures were calculated within the LSDA framework to analyze these modifications in detail. As expected, bulk SiC is a wide-band-gap material, although standard LSDA calculations typically underestimate the gap. In our case, LSDA yields direct and indirect band gaps of approximately 3.8 eV and 2.1 eV, respectively, compared to the experimental value of ~3.33 eV. To improve the description of localized electronic interactions, the LSDA+U approach was employed. With the inclusion of on-site Coulomb corrections, the calculated gaps increase to about 5.2 eV (direct) and 3.3 eV (indirect), showing better agreement with available experimental and theoretical data. Al

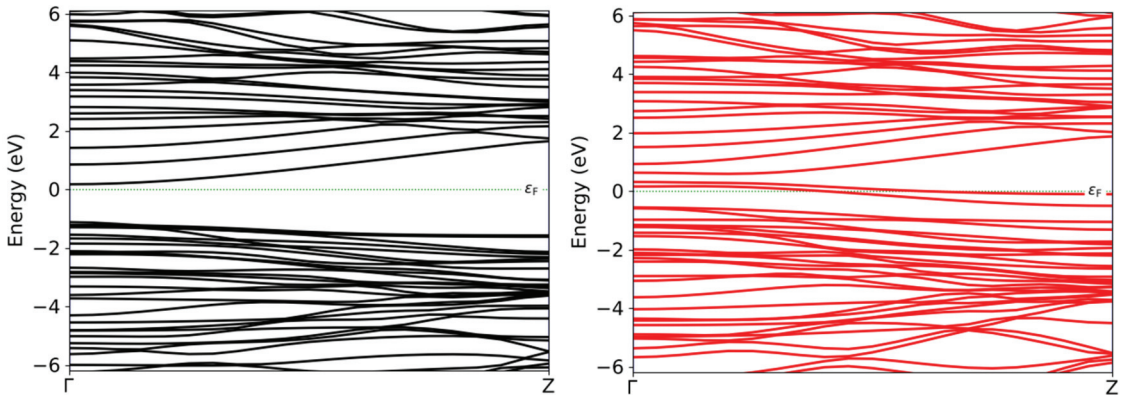

Fig. 2. The calculated spin-up (black) and spin-down (red) band structures for Al@Si-doped (6,0) SWSiCNT systems.

substitution introduces impurity states close to the Fermi level, leading to a substantial rearrangement of the electronic bands. The spin-up channel remains semiconducting, though with a reduced band gap of around 1.3 eV. In contrast, the spin-down channel becomes metallic due to the disappearance of the gap. This spin-dependent behavior suggests the onset of half-metallicity, a property that is particularly attractive for spintronic applications since it enables spin-polarized charge transport. The electronic behavior of the Al-substituted (6,0) SiC nanotube can be better understood through the analysis of the total density of states (TDOS) and the spin-resolved band dispersion presented in Figures 2 and 3, respectively.

The TDOS profile clearly demonstrates a strong imbalance between the two spin channels. The Fermi level is positioned at 0 eV and separates occupied from unoccupied states. For the spin-up component, a distinct energy gap persists at the Fermi level, indicating semiconducting behavior. In contrast, the spin-down channel shows a nonzero density of states at the Fermi level, evidencing metallic conductivity. This pronounced spin asymmetry is a hallmark of half-metallicity, where charge transport is allowed for only one spin orientation. Such a property is highly desirable for spintronic applications because it enables intrinsically spin-polarized current without the need for external filtering mechanisms.

The TDOS peaks in the vicinity of the Fermi energy originate from orbital mixing between carbon p states and aluminum d states. This hybridization substantially modifies the local electronic environment around the dopant atom and plays a decisive role in shaping the spin-dependent electronic structure. The band

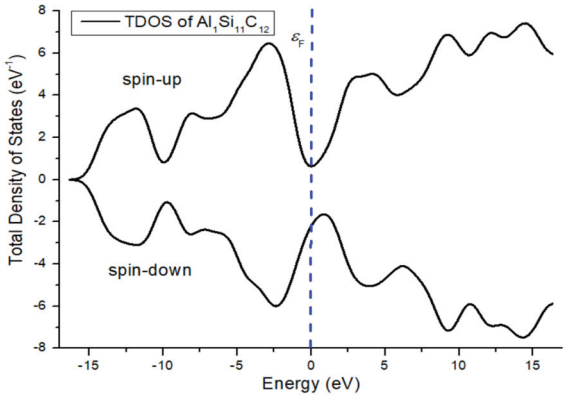

Fig. 3. The calculated spin-polarized TDOS for Al@Si-doped (6,0) SWSiCNT systems.

structure analysis further confirms these observations. In the spin-up channel, an energy gap of approximately 1.3 eV is preserved, consistent with semiconducting characteristics. Conversely, the spin-down bands intersect the Fermi level, producing a metallic dispersion. The band crossings occur near the Γ point, leading to gap closure and an enhanced density of states around the Fermi energy. This behavior explains the improved electrical conductivity in the doped system. Partial density of states (PDOS) calculations reveal that states near the Fermi level are mainly derived from carbon 2p orbitals with significant contributions from aluminum d orbitals. The interaction between these orbitals induces spin polarization and stabilizes the half-metallic state. The reduction of the spin-down band gap to zero is therefore directly linked to dopant-induced orbital hybridization.

Overall, the combined TDOS, PDOS, and band structure results demonstrate that substitutional aluminum introduces pronounced spin asymmetry into the SiC nanotube lattice. The emergence of half-metallicity, driven by

p–d orbital coupling, suggests that Al-doped SiC nanotubes may serve as promising building blocks for nanoscale spintronic components such as spin filters and magnetic junction devices.

*3.2 Magnetic characteristics of SW*SiC*: Al nanotubes*

The Mulliken population analysis reveals that Al substitution induces a total magnetic moment of approximately 1.0 μB in the (6,0) SiC nanotube. This magnetization originates from spin imbalance created by the replacement of a Si atom with Al, which perturbs the local electronic structure and breaks spin symmetry.

The calculated spin density distribution shows that the magnetism is not uniformly distributed across the nanotube but is mainly concentrated around the dopant site. The nearest carbon atoms exhibit pronounced positive spin polarization, indicating that they play a dominant role in stabilizing the magnetic state. Their enhanced magnetic response can be attributed to strong electronic interaction with the Al impurity.

In contrast, the aluminum atom carries a negative spin magnetic moment, implying antiparallel alignment relative to the surrounding carbon atoms. This behavior suggests antiferromagnetic coupling between the dopant and its nearest neighbors. Nearby silicon atoms also contribute small negative spin moments, partially compensating the positive polarization of carbon atoms. As the distance from the dopant increases, the spin polarization gradually diminishes and the atomic magnetic moments approach negligible values, confirming the localized character of the induced magnetism.

Orbital-resolved Mulliken analysis provides further insight into the microscopic origin of this magnetic behavior. For silicon atoms, spin polarization mainly arises from the 3p orbitals, with smaller contributions from 3s states and minor participation of d-like orbitals, indicating moderate hybridization effects. Carbon atoms display stronger and more localized polarization, predominantly associated with their 2p orbitals, while 2s and d-like contributions remain comparatively weak. The aluminum dopant shows significant spin imbalance primarily in its 3p orbitals, which are strongly hybridized with the neighboring carbon 2p states. This p–p interaction is the key factor driving the emergence of magnetism in the doped system. Additional, though smaller, contributions

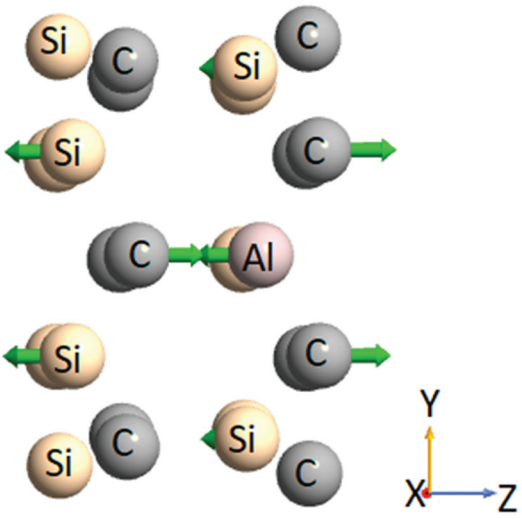

Fig. 4. Spin polarization in Al@Si-doped SiC nanotubes. The green arrows indicate the local magnetic moments.

from Al 3s and d-like states further modulate the magnetic response.

The presence of spin polarization in d-like orbitals across the structure indicates that hybridization extends beyond simple s–p interactions, contributing to the redistribution of electronic charge and stabilization of the magnetic configuration. The resulting total magnetic moment is therefore the cumulative effect of these orbital contributions, consistent with an overall antiferromagnetic coupling pattern in the Al-doped nanotube.

Figure 4 illustrates the spatial distribution of spin polarization for Al@Si-doped in (6,0) SWSiCNT. The vectors indicate both the magnitude and orientation of local magnetic moments. The carbon atoms closest to the dopant exhibit strong positive spin alignment, whereas the aluminum atom shows an oppositely oriented (negative) moment. This antiparallel arrangement confirms the localized antiferromagnetic interaction between the dopant and its neighboring atoms. Overall, the magnetic state of the Al@Si-doped SiC nanotube emerges from localized dopant-induced spin polarization mediated by orbital hybridization, highlighting its potential relevance for nanoscale spin-dependent transport applications.

Silicon atoms located farther from the impurity site also develop small spin moments oriented opposite to the dominant polarization direction. Although their magnitudes are weaker compared to the nearest carbon atoms, their antiparallel alignment further supports the presence of antiferromagnetic coupling

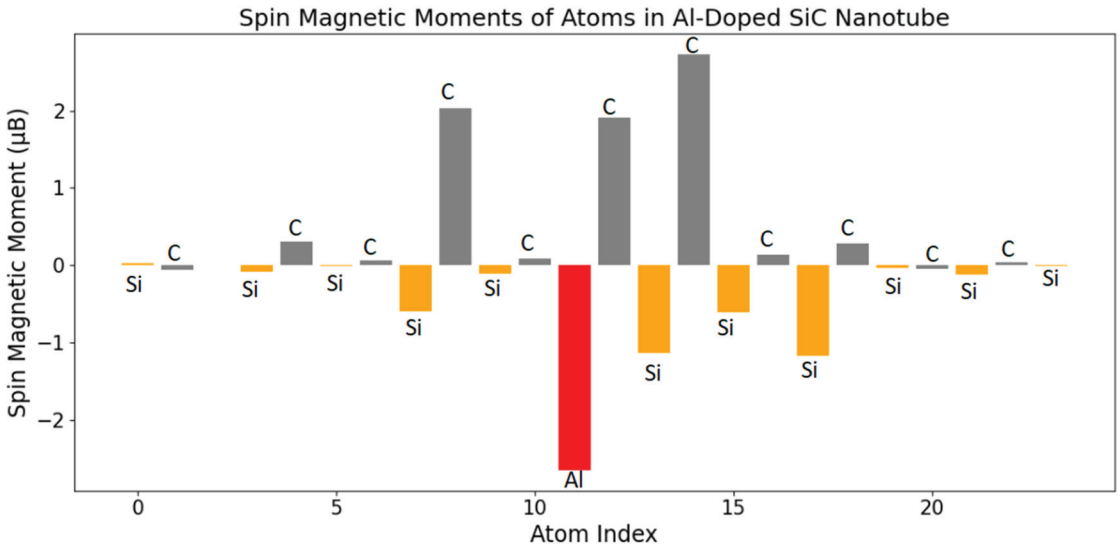

Fig. 5. Spin magnetic moments for individual atoms in the Al@Si-doped (6,0) SiC nanotube.

throughout the nanotube. The spatial distribution and systematic orientation of the spin vectors indicate that Al substitution breaks the intrinsic spin symmetry of the pristine structure, producing localized spin polarization centered on the dopant region.

The resulting magnetic arrangement is therefore consistent with an antiferromagnetic ground state. This conclusion agrees with both the Mulliken population analysis and the total energy calculations performed for different magnetic configurations, confirming that the antiferromagnetic ordering is energetically favorable in the Al@Si-doped SiC nanotube.

Figure 5 displays the calculated distribution of atomic spin magnetic moments in the Al-doped SiC nanotube. The results are obtained from spin-polarized DFT calculations combined with Mulliken population analysis. Each column in the bar diagram corresponds to an individual atom, identified by its atomic index along the horizontal axis, while the vertical axis represents the magnitude of the magnetic moment expressed in Bohr magnetons (μ_B).

This representation provides a clear visualization of how the magnetic response varies from atom to atom within the nanotube, highlighting the localized influence of the aluminum dopant on the surrounding lattice.

The color coding reflects the atomic species:

Gray bars (C atoms): Many carbon atoms exhibit significant positive spin moments, especially those directly bonded to the Al dopant. These atoms are the primary contributors to the total magnetic moment of the system.

Orange bars (Si atoms): Most silicon atoms show small or moderate negative spin moments, indicating antiferromagnetic alignment with the positively polarized carbon atoms.

Red bar (Al atom): The Al dopant shows a large **negative** magnetic moment (~–2.64 [μ_B]), consistent with its role in inducing strong spin polarization and participating in antiferromagnetic coupling.

The bar diagram further confirms that the largest positive spin moments are concentrated on the carbon atoms adjacent to the Al impurity, whereas the Al atom and several neighboring Si atoms carry negative spin moments. This opposite alignment clearly indicates antiferromagnetic coupling and demonstrates that the magnetic response remains strongly localized around the dopant site rather than being uniformly distributed throughout the nanotube.

Table 1 compiles the principal electronic and magnetic parameters obtained from first-principles calculations for the Al-doped (6,0) SiC nanotube. The calculated spin-resolved band structure evidences half-metallic behavior, arising from dopant-induced asymmetry between the two spin channels. The coexistence of metallic conduction in one spin channel and a finite gap in the other, together with localized spin polarization near the Al atom, underscores the spin-selective transport characteristics of the system.

Analysis of the total spin distribution shows that the magnetic moment is primarily confined to the Al atom and its nearest carbon neighbors. The net magnetic moment of approximately 1.0

Table 1. Summary of electronic and magnetic properties of Al@Si-doped (6,0) SWSiCNT.

Property	Value / Description
Structure type	Single-walled (6,0) SiC nanotube (SWSiCNT)
Bond length (Si–C)	~[1.88 Å]
Tube radius	~[3.11 Å]
Doping type	Substitutional doping of Si atom by Al
Exchange-correlation functional	LSDA + Hubbard U correction (LSDA+U)
Corrected band gaps (bulk SiC)	5.2 [eV] (direct), 3.3 [eV] (indirect
Band gap (spin-up channel)	~1.3 [eV] (semiconducting)
Band gap (spin-down channel)	0 [eV] (metallic)
Electronic behavior	Half-metallic (metallic in one spin channel, semiconducting in the other)
Fermi level contribution	Dominated by hybridized Al 4d and C 2p orbitals
Density of states (DOS)	Spin-asymmetric; metallic behavior in spin-down channel
Spin magnetic moment (total)	~1.0 [μ_B]
Magnetization origin	Strong positive spin moments from C atoms near Al dopant; negative moment on Al atom
Spin moment of Al dopant	~–2.64 [μ_B](negative)
Magnetic coupling	Antiferromagnetic (AFM) alignment between Al and neighboring Si, C atoms
Magnetic ground state	AFM more stable than FM by ~21.0452 [eV]
Orbital contributions (dominant)	C: 2p orbitals; Si: 3p orbitals; Al: 3p and 4d orbitals
Spin localization	Strongly localized around Al dopant and adjacent carbon atoms
Potential applications	Spin filters, magnetic memory, spin injectors, nano-optoelectronics

μ_B indicates incomplete compensation between spin-up and spin-down electron populations. This imbalance is consistent with the half-metallic character identified in the electronic structure calculations and reinforces the magnetic functionality of the doped nanotube.

To establish the magnetic ground state, total energies were evaluated for both ferromagnetic (FM) and antiferromagnetic (AFM) configurations. The AFM configuration exhibits a lower total energy (−3912.51781 eV) compared to the FM state (−3891.47261 eV), demonstrating that antiferromagnetic ordering is energetically favored. The substantial energy difference confirms that the AFM state represents the true ground state of the Al-doped (6,0) SiC nanotube.

These results collectively highlight the strong interplay between orbital hybridization, spin polarization, and magnetic ordering in the doped system. The combination of structural stability, half-metallic character, and an energetically stable antiferromagnetic state suggests that Al-doped SiC nanotubes may serve as promising building blocks for advanced nanoscale spintronic and antiferromagnetic device architectures.

4. Conclusion

In this study, the electronic and magnetic properties of aluminum-silicon substituted (6,0) single-walled SiC nanotubes were systematically investigated using spin-polarized density functional theory. The substitution of a Si atom by Al introduces significant spin asymmetry in the electronic structure, giving rise to half-metallic behavior characterized by metallic conduction in one spin channel and semiconducting behavior in the other.

Spin density and Mulliken population analyses reveal a total magnetic moment of approximately 1.0 μ_B, primarily originating from carbon atoms directly bonded to the dopant. The aluminum atom exhibits antiparallel spin alignment relative to its neighbors, leading to an overall antiferromagnetic coupling pattern. Total energy comparisons confirm that the antiferromagnetic configuration is energetically more stable than the ferromagnetic one, identifying it as the magnetic ground state.

Overall, the tunable half-metallicity, localized spin polarization, and stable antiferromagnetic ordering demonstrate the potential of Al@Si-doped SiC nanotubes for future spin-dependent nanoelectronic applications, including spin filters, spin injectors, and antiferromagnetic memory elements.

References

1. Zhang W., Zhang F., Zhang Z., Lu S., Yang Y., Sci. China Phys. Mech. 53, 1582 (2010). https://doi.org/10.1007/s11433-010-4089-8
2. Madar R., Nature 430, 974 (2004). https://doi.org/10.1038/430974a
3. Alam K. M., Ray A. K., Phys. Rev. B 77, 035436 (2008). https://doi.org/10.1103/PhysRevB.77.035436
4. Baumeier B., Krüger P., Pollmann J., Phys. Rev. B 76, 085407 (2007). https://doi.org/10.1103/PhysRevB.76.085407
5. Ponraj J. S., Dhanabalan S. C., Attolini G., Salviati G., Crit. Rev. Solid State Mater. Sci. 41, 430 (2016). https://doi.org/10.1080/10408436.2016.1150806
6. Santos E., Ayuela A., Sanchez-Portal D., New J. Phys. 12, 053012 (2010). https://doi.org/10.1088/1367-2630/12/5/053012
7. Zhao J. X., Ding Y. H., J. Phys. Chem. C 112, 2558 (2008). https://doi.org/10.1021/jp073722m
8. Heidarzadeh H., Opt. Quant. Electron. 51, 32 (2019). https://doi.org/10.1007/s11082-019-1742-y
9. Mulatu A. T., Nigussa K. N., Deja L. D., Optical Mater. 134, 113094 (2022). https://doi.org/10.1016/j.optmat.2022.113094
10. Vatankhah Ch., Badehian H. A., Optik 237, 166740 (2021). https://doi.org/10.1016/j.ijleo.2021.166740
11. Ibaeva R. Z., Jafarova V. N., Eminova V. I., Scurtu I. C., Lupu S., J. Nanopart. Res. 26, 23 (2024). https://doi.org/10.1007/s11051-024-06109-w
12. Asadullayeva S. G., Jahangirli Z. A., Eur. Phys. J. B 98, 142 (2025).
10.1140/epjb/s10051-025-00990-7
13. Jafarova V. N., Eminova V. I., Musaev M. A., Scurtu I. C., Technium 26, 1 (2025). https://doi.org/10.47577/technium.v26i.12149
14. Tien N. T., Thao P. T. B., Jafarova V. N., Roy D. D., Silicon, 1 (2024). https://doi.org/10.1007/s12633-024-03127-0
15. Rzayeva S., Jafarova V. N., Roy D. D., Mater. Sci. Semicond. Process. 197, 109702 (2025). https://doi.org/10.1016/j.mssp.2025.109702
16. Rzayeva S., Jafarova V. N., Turkish Comput. Theor. Chem. 9, 112 (2025). https://doi.org/10.33435/tcandtc.1535679
17. Rzayeva S., Jafarova V. N., J. Polytechnic 28, 947 (2025). https://doi.org/10.2339/politeknik.1536597
18. Wu A. Q., Song Q. G., Yang L., Adv. Mater. Res. 510, 747 (2012). https://doi.org/10.4028/www.scientific.net/AMR.510.747
19. Kohn W., Sham L. J., Phys. Rev. 140, A1133 (1965). https://doi.org/10.1103/PhysRev.140.A1133
20. Cococcioni M., de Gironcoli S., Phys. Rev. B 71, 035105 (2005). https://doi.org/10.1103/PhysRevB.71.035105